

# Nucleon Axial Charge in (2 + 1)-Flavor Dynamical-Lattice QCD with Domain-Wall Fermions

T. Yamazaki,<sup>1</sup> Y. Aoki,<sup>2</sup> T. Blum,<sup>1,2</sup> H. W. Lin,<sup>3</sup> M. F. Lin,<sup>4</sup> S. Ohta,<sup>5,6,2</sup> S. Sasaki,<sup>7</sup> R. J. Tweedie,<sup>8</sup> and J. M. Zanotti<sup>8</sup>

(RBC+UKQCD Collaborations)

<sup>1</sup>Physics Department, University of Connecticut, Storrs, Connecticut, 06269-3046, USA

<sup>2</sup>RIKEN-BNL Research Center, Brookhaven National Laboratory, Upton, New York 11973, USA

<sup>3</sup>Thomas Jefferson National Accelerator Facility, Newport News, Virginia 23606, USA

<sup>4</sup>Center for Theoretical Physics, Massachusetts Institute of Technology, Cambridge, Massachusetts 02139, USA

<sup>5</sup>Institute of Particle and Nuclear Studies, KEK, Tsukuba, 305-0801, Japan

<sup>6</sup>Physics Department, Sokenai Graduate U. Adv. Studies, Hayama, Kanagawa 240-0193, Japan

<sup>7</sup>Department of Physics, University of Tokyo, Hongo 7-3-1, Bunkyo-ku, Tokyo 113, Japan

<sup>8</sup>School of Physics, The University of Edinburgh, Edinburgh EH9 3JZ, United Kingdom

(Received 25 January 2008; published 28 April 2008)

We present results for the nucleon axial charge  $g_A$  at a fixed lattice spacing of  $1/a = 1.73(3)$  GeV using 2 + 1 flavors of domain wall fermions on size  $16^3 \times 32$  and  $24^3 \times 64$  lattices ( $L = 1.8$  and  $2.7$  fm) with length 16 in the fifth dimension. The length of the Monte Carlo trajectory at the lightest  $m_\pi$  is 7360 units, including 900 for thermalization. We find finite volume effects are larger than the pion mass dependence at  $m_\pi = 330$  MeV. We also find a scaling with the single variable  $m_\pi L$  which can also be seen in previous two-flavor domain wall and Wilson fermion calculations. Using this scaling to eliminate the finite-volume effect, we obtain  $g_A = 1.20(6)(4)$  at the physical pion mass,  $m_\pi = 135$  MeV, where the first and second errors are statistical and systematic. The observed finite-volume scaling also appears in similar quenched simulations, but disappear when  $V \geq (2.4 \text{ fm})^3$ . We argue this is a dynamical quark effect.

DOI: 10.1103/PhysRevLett.100.171602

PACS numbers: 12.38.Gc, 11.15.Ha, 11.30.Rd, 12.38.Aw

The isovector axial charge of nucleon is a fundamental observable in hadron physics. It is defined as the axial vector form factor at zero four-momentum transfer,  $g_A = G_A(0)$ . The axial vector form factor is given by the nucleon matrix element of the axial vector current,  $A_\mu^a = \bar{\psi} \gamma_\mu \gamma_5 (\tau^a/2) \psi$ , with  $u, d$  quark doublet  $\psi$ ,  $\langle n' | A_\mu^a | n \rangle = \bar{u}_n' [\gamma_\mu G_A(q^2) + i q_\mu G_P(q^2)] \gamma_5 (\tau^a/2) u_n$ , where  $G_P$  is the induced pseudoscalar form factor,  $\tau^a$  an isospin Pauli matrix, and  $q$  the momentum transfer,  $q_\mu = p_\mu^n - p_\mu^{n'}$ . Experimentally,  $g_A$  has been obtained very precisely,  $g_A = 1.2695(29)$  [1], through neutron  $\beta$  decay.

$g_A$  is related to the spontaneous breaking of the chiral symmetry of the strong interaction through the well-known Goldberger-Treiman relation [2]. This relation shows that  $g_A$  is proportional to the strong pion-nucleon coupling at  $q^2 \approx 0$ . Furthermore, the Adler-Weisberger sum rule [3,4] reveals that  $g_A$  differs from unity for a structureless nucleon through the difference between the integrals of the total cross sections of the  $\pi^+ p$  and  $\pi^- p$  channels. These are in good agreement with experiments.

Hence the axial charge allows us to perform a precision test of (lattice) QCD in the baryon sector. Moreover, since it is an isovector matrix element, only connected quark diagrams at  $q^2 = 0$  contribute, making the calculation technically simpler. Furthermore, the renormalization of the axial vector current is simplified when utilizing a lattice chiral fermion action such as the domain-wall fermion (DWF) action [5–7]. However, it is difficult to control

finite-volume effects (FVE's) in  $g_A$ , as suggested by quenched calculations [8]. The FVE's have been investigated in effective models [9,10], and also in heavy baryon chiral perturbation theory (HBChPT) [11–13]. The FVE's in HBChPT are inconsistent with lattice calculations unless contributions of the  $\Delta$  baryon resonance are included. Such contributions introduce several unknown parameters, and the FVE seems sensitive to one of them, the  $\Delta - N$  coupling [11,13,14]. Until now, there has been only one investigation in the light quark mass region with 2 + 1 flavors, the mixed action calculation [15] by LHPC which reported the FVE is small for a volume of  $V = (2.5 \text{ fm})^3$ .

In this Letter, we report a result for  $g_A$  using 2 + 1 flavors of dynamical DWF with several quark masses corresponding to  $m_\pi = 0.33\text{--}0.67$  GeV, on two volumes with spatial size  $L = 1.8$  and  $2.7$  fm. Our light quark masses and the spatial volumes allow a detailed investigation of the FVE in full QCD where the sea and valence quarks are identical. It is found that the FVE is not negligible at the lightest  $m_\pi$ , even on the larger volume, and that  $g_A$  exhibits a scaling behavior with the single variable  $m_\pi L$ .

Our calculation is performed with a fixed lattice spacing, two space-time lattice sizes,  $16^3 \times 32$  and  $24^3 \times 64$ , the Iwasaki gauge action [16] with  $\beta = 2.13$ , and the DWF action with a fifth dimension of size 16 and  $M_5 = 1.8$ . Each ensemble of configurations uses the same dynamical strange quark mass,  $m_s^{\text{sea}} = 0.04$  in lattice units. We use

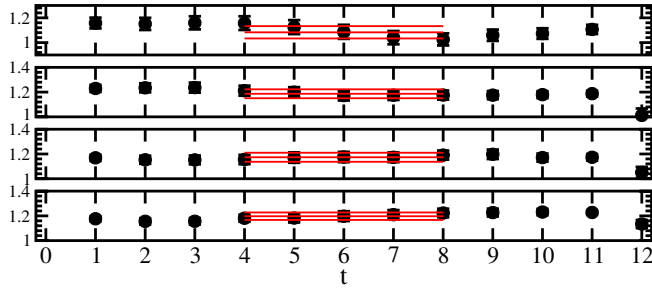


FIG. 1 (color online). Plateaus of  $g_A$ .  $V = (2.7 \text{ fm})^3$  and  $m_f = 0.005, 0.01, 0.02$ , and  $0.03$ , from top to bottom.

four light sea quark masses on the  $24^3$  lattice,  $m_{\text{sea}} = 0.005, 0.01, 0.02$ , and  $0.03$  and the same heaviest three masses on the  $16^3$  lattice. The ensembles, described in [17,18], were generated using the RHMC algorithm [19] with trajectories of unit length. The measurements were performed at the unitary points only,  $m_f = m_{\text{val}} = m_{\text{sea}}$ . We use the mass of the  $\Omega^-$  baryon to determine the inverse of the lattice spacing  $1/a = 1.73(3) \text{ GeV}$  [20,21]. The residual quark mass due to the finite size of the fifth dimension is  $0.00315(2)$ . The nonzero lattice spacing error is small in our calculation because the DWF action is automatically off-shell  $O(a)$  improved.

Four measurements are carried out for the  $24^3$  ensembles on each configuration. The number of Monte Carlo trajectories used for measurements is 6460, 3560, 2000, and 2120 for  $m_f = 0.005, 0.01, 0.02, 0.03$ , respectively, with 10 trajectory separations for  $m_f = 0.005, 0.01$  and 20 for  $0.02, 0.03$ . The measurements are blocked into bins of 40 trajectories each to reduce autocorrelations. On the  $16^3$  ensembles, we use 3500 trajectories separated by 10 trajectories at  $m_f = 0.01$ , and  $0.03$ , and by 5 at  $0.02$ . The data are blocked with 20 trajectories per bin.

The axial charge is calculated from the ratio of the matrix elements of the spatial component of the axial vector current and the temporal component of the vector current,  $V_t^a = \bar{\psi} \gamma_t (\tau^a/2) \psi$ ,  $\langle n' | A_i^a | n \rangle / \langle n' | V_t^a | n \rangle = g_A$ . This ratio gives the renormalized axial charge because  $A_\mu$  and  $V_\mu$  share a common renormalization constant due to the chiral symmetry of DWF. In our simulation, the two constants are consistent to less than 0.5% at the chiral limit. In order to increase the overlap with the ground state, the quark propagators are calculated with gauge invariant Gaussian smearing [22], and we employ sufficient separation in Euclidean time, more than 1.37 fm, which is the largest used so far in dynamical calculations of  $g_A$  [15,23,24], between the location of the nucleon source and sink to minimize excited state contamination.

The plateaus of  $g_A$  computed on volume  $V = (2.7 \text{ fm})^3$  are shown in Fig. 1. We checked that consistent results are obtained by either fitting or averaging over appropriate time slices,  $t = 4-8$ , and also by fitting the data symmetrized about  $t = 6$ . The larger volume data can be symme-

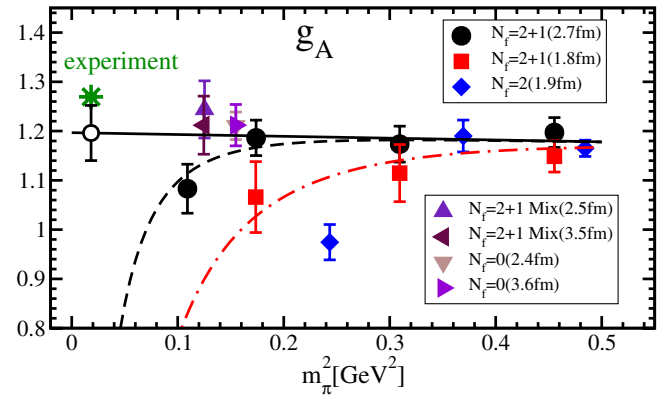


FIG. 2 (color online).  $g_A$ . Dashed and solid lines denote the fit results and chiral extrapolation in infinite volume, respectively. The open circle is extrapolated result at  $m_\pi = 135 \text{ MeV}$ .

trized because the source and sink operators are identical in the limit of large statistics. We note that the length of our lightest mass run is already the longest we know of for comparable simulation parameters. Results obtained from the fit using the unsymmetrized data, presented in the figure with 1 standard deviation, are employed in the analysis.

Figure 2 shows our result for  $g_A$ . The results are also presented in Table I. The  $(2.7 \text{ fm})^3$  data are almost independent of the pion mass (squared) except for the lightest point which is about 9% smaller than the others. A set of the results obtained with a smaller volume,  $(1.8 \text{ fm})^3$ , shows a similar downward behavior, albeit with relatively larger statistical uncertainties. An earlier two-flavor calculation by RBC [14] with spatial volume  $(1.9 \text{ fm})^3$ , and  $1/a = 1.7 \text{ GeV}$  showed a clear downward behavior, but it sets in at heavier pion mass.

We suspect that this pion mass dependence driving  $g_A$  away from the experimental value is caused by the finite volume of our calculation: in general, such an effect is expected to grow as the quark mass gets lighter at fixed volume, or the volume decreases for fixed quark mass. More quantitatively, we observe in the figure that the two-flavor result with  $V = (1.9 \text{ fm})^3$  significantly decreases at  $m_\pi^2 \approx 0.24 \text{ GeV}^2$ , while the  $2 + 1$  flavor results with  $V = (2.7 \text{ fm})^3$  do not decrease even at  $m_\pi^2 \approx 0.17 \text{ GeV}^2$ . Another trend of the FVE seen in Fig. 2 is that all the  $2 + 1$  flavor, smaller volume data are systematically lower than the larger volume data. Similar behavior was observed in quenched DWF studies [8,25].

TABLE I.  $g_A$  and  $m_\pi$  [ $V = (2.7 \text{ fm})^3$  only].

$m_f$	0.005	0.01	0.02	0.03
$m_\pi$ [GeV][21]	0.3313(13)	0.4189(13)	0.5572(5)	0.6721(6)
$(2.7 \text{ fm})^3$	1.083(50)	1.186(36)	1.173(36)	1.197(30)
$(1.8 \text{ fm})^3$	N/A	1.066(72)	1.115(58)	1.149(32)

However, for pion masses close to our lightest point, such a sizable shift is not observed when  $V$  is larger than about  $(2.4 \text{ fm})^3$ , not only in the quenched case, but also the  $2 + 1$  flavor, mixed action, calculation in [15], as shown in Fig. 2. On the other hand, our results suggest that  $V = (2.7 \text{ fm})^3$  is not enough to avoid a significant FVE on  $g_A$  when  $m_\pi \leq 0.33 \text{ GeV}$  in dynamical fermion calculations.

In order to more directly compare the various results, we plot  $g_A$  against a dimensionless quantity,  $m_\pi L$ , in the top panel of Fig. 3. Interestingly, we find that the  $2 + 1$  flavor results on both volumes and the two-flavor ones reasonably collapse onto a single curve that monotonically increases with  $m_\pi L$ ; in other words, they exhibit scaling in  $m_\pi L$ . A similar scaling also appears in dynamical two-flavor (improved) Wilson fermion calculations as shown in the middle panel of Fig. 3 [13,23,24] for the unitary points  $\kappa_{\text{sea}} = \kappa_{\text{val}}$ , with various volumes  $(0.95\text{--}2.0 \text{ fm})^3$ , pion masses  $0.38\text{--}1.18 \text{ GeV}$ , and gauge couplings. The large difference in Wilson data at  $\beta = 5.60$  on  $m_\pi L \sim 6.5$  can be described by different choices of the renormalization constant of  $A_\mu$ . While the trend is similar in the quenched DWF case [8,25] with pion masses in the range  $0.39\text{--}0.86 \text{ GeV}$  and  $1/a = 1.3 \text{ GeV}$  (see bottom panel, Fig. 3), the scaling is violated for the point with smallest  $m_\pi L$  on  $V = (2.4 \text{ fm})^3$ . The lightest point does not follow the  $(1.8 \text{ fm})^3$  data: they differ by 2.5 standard deviations ( $\sigma$ ) at  $m_\pi L \sim 5$ , suggesting that there are nonuniversal terms that depend separately on  $m_\pi$  and  $V$ . In particular, this

effect may be due to the presence of a quenched chiral log [26]. From [26], the size of the effect at this mass can readily explain the discrepancy observed with the dynamical  $m_\pi L$  scaling. Note, at this mass, but going to  $V = (3.6 \text{ fm})^3$ , no FVE is detected in the quenched case as can be seen in Fig. 2.

It is interesting to compare our larger volume,  $2 + 1$  flavor result with the mixed action,  $2 + 1$  flavor result with a similar volume [15], denoted by the left triangle in the top panel of Fig. 3. At heavy pion mass, the results are statistically consistent and essentially independent of  $m_\pi L$ . At  $m_\pi L \sim 4.5$ , the mixed action result, however, is larger than ours by (a combined)  $2.1\sigma$ , but consistent with the quenched DWF result with  $(2.4 \text{ fm})^3$  volume [8] (the up triangle in the figure), which is also  $2.2\sigma$  larger than our result. The mixed action result was also calculated with an even larger volume, and no FVE was detected [15]. Again, similar to the quenched case.

A possible explanation of the difference is that it is simply a dynamical fermion effect. The mixed action results are partially quenched, calculated with improved staggered sea quarks and domain-wall valence quarks. The pion mass of valence DWF is tuned to match the lightest pseudoscalar meson mass computed entirely with staggered fermions. However, there is an ambiguity [27,28] in choosing the staggered pseudoscalar meson for this tuning since there are several. Thus, if the valence quark is effectively much lighter than the sea quark, a mixed action calculation effectively becomes quenched. This may lead to a deviation from the unitary calculation and consistency with the quenched calculation. Mixed action ChPT shows the presence of partially quenched logs whose size is consistent with the observed effect [29,30].

For the chiral extrapolation of  $g_A$ , we attempt to include the FVE in our data. While the pion mass dependence of  $g_A$ , including the FVE, has been investigated in the small scale expansion (SSE) scheme of HBChPT [13], the size of the FVE on  $V = (2.7 \text{ fm})^3$  predicted in SSE is less than 1% in our pion mass region. The correction is much too small to account for the observed FVE in our data. This suggests that the FVE in HBChPT, which is estimated by replacing all loop integrals by summations, is not the leading FVE in  $g_A$ , as one in  $\epsilon$  regime [31]. We also note that our attempts to fit the mass dependence of the data to HBChPT failed, which is likely due to the heavier quark mass points being beyond the radius of convergence of ChPT [20,21,32].

Instead of the SSE formula, we assume the following simple fit form, including the FVE in a way that respects the scaling observed in the data,  $A + Bm_\pi^2 + Cf_V(m_\pi L)$ , with  $f_V(x) = e^{-x}$ , and where  $A$ ,  $B$ , and  $C$  are fit parameters. We employ a constant term and one linear in the pion mass squared, the leading contributions to  $g_A$  in infinite volume. The third term corresponds to the observed FVE, taken as a function of  $m_\pi L$  only, and vanishes rapidly towards the infinite volume limit,  $L \rightarrow \infty$  at fixed pion

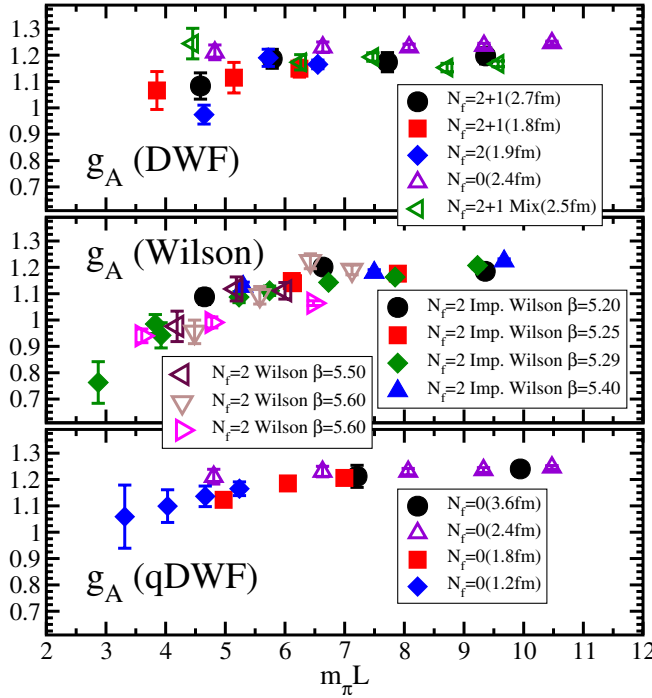


FIG. 3 (color online).  $m_\pi L$  scaling of  $g_A$ . Top, middle, and bottom panels are dynamical and mixed action DWF, dynamical Wilson, and quenched DWF results, respectively. In the bottom panel, open symbol is same as in the top panel.

mass. The same  $m_\pi L$  dependence appears in one of the FVE contributions in Ref. [9]. We note that this simple form is used to estimate the FVE's in the data but *not* the value of  $g_A$  in the chiral limit at fixed  $L$ . In the end, we chose this simplest form, in part, because the fit result at the physical point is not sensitive to the particular choice of  $f_V(x)$ , as discussed below.

In Fig. 2, we see that the  $2 + 1$  flavor data are described very well by this simple fit ( $\chi^2/\text{d.o.f.} = 0.45$ ), using data computed on both volumes simultaneously. The  $L \rightarrow \infty$  extrapolation (solid line) in turn allows an extrapolation to the physical pion mass ( $m_\pi = 135$  MeV),  $g_A = 1.20(6)(4)$ , where the first error is statistical. The second error is an estimate of the systematic error determined by comparing this result with that from fits using different choices of  $f_V(x)$ , *e.g.*, the full form in [9],  $x^{-3}$ , and  $m_\pi^2 e^{-x}/x^{1/2}$ . The latter is similar to HBChPT when  $m_\pi L \gg 1$  [11–13]. The extrapolated value is not sensitive to the choice of  $f_V$  and is also consistent with a linear fit to the three heaviest points on the larger volume,  $g_A = 1.17(6)$ . We also fit our data, with and without the  $f_V$  term, to the 2-loop formula from HBChPT [32] and find that the extrapolated result is less than 1 and that the fits are generally unstable. This is because the many unknown low energy constants cannot be determined well from only four data points, even if some of them are fixed. More importantly, though the 2-loop formula extends the range of the chiral expansion, it is still only large enough to include our lightest point, as demonstrated in Ref. [32]. The systematic error arising from the difference of the renormalization constants for  $A_\mu$  and  $V_\mu$  is much smaller than the quoted systematic error. From the fit result with  $f_V(x) = e^{-x}$ , we estimate that if one aims to keep FVE's at or below 1%, then for  $m_\pi = 330$  MeV, spatial sizes of 3.4–4.1 fm ( $m_\pi L \approx 5.7$ –6.9) are necessary.

We have computed the nucleon axial charge with  $2 + 1$  flavors of DWF on a largest volume of  $(2.7 \text{ fm})^3$ , a lightest  $m_\pi$  of 330 MeV, and large statistics. We have observed a downward  $m_\pi$  dependence of  $g_A$  on our larger volume, and by comparing our results with those using different volumes, numbers of flavors, and lattice fermions as a function of the single variable  $m_\pi L$ , concluded it is caused by the finite volume used in our calculation. The data appear to scale well in this variable except in the quenched and partially quenched, mixed action cases when the volume exceeds roughly  $(2.4 \text{ fm})^3$ , which may be due to the presence of (partially) quenched chiral logs.

We thank our colleagues in the RBC and UKQCD collaborations for helpful discussions. We thank Columbia University, University of Edinburgh, PPARC, RIKEN, BNL, and the U.S. DOE for providing the QCDOC supercomputers used in this work. T.B. and

T.Y. were supported by the U.S. DOE under Contract No. DE-FG02-92ER40716. H.L. is supported by DOE Contract No. DE-AC05-06OR23177 under which JSA, LLC operates THNAF. S.S. is supported by JSPS No. (19540265). J.Z. is supported by PPARC Grant No. PP/D000238/1.

- 
- [1] W.-M. Yao *et al.*, J. Phys. G **33**, 1 (2006).
  - [2] M. L. Goldberger and S. B. Treiman, Phys. Rev. **110**, 1178 (1958).
  - [3] W. I. Weisberger, Phys. Rev. Lett. **14**, 1047 (1965).
  - [4] S. L. Adler, Phys. Rev. Lett. **14**, 1051 (1965).
  - [5] D. B. Kaplan, Phys. Lett. B **288**, 342 (1992).
  - [6] Y. Shamir, Nucl. Phys. B **406**, 90 (1993).
  - [7] V. Furman and Y. Shamir, Nucl. Phys. B **439**, 54 (1995).
  - [8] S. Sasaki *et al.* (RBCK Collaboration), Phys. Rev. D **68**, 054509 (2003).
  - [9] R. L. Jaffe, Phys. Lett. B **529**, 105 (2002).
  - [10] A. W. Thomas *et al.*, J. Phys. Conf. Ser. **9**, 321 (2005).
  - [11] S. R. Beane and M. J. Savage, Phys. Rev. D **70**, 074029 (2004).
  - [12] W. Detmold and C.-J. D. Lin, Phys. Rev. D **71**, 054510 (2005).
  - [13] A. Ali Khan *et al.* (QCDSF Collaboration), Phys. Rev. D **74**, 094508 (2006).
  - [14] H.-W. Lin *et al.*, arXiv:0802.0863.
  - [15] R. G. Edwards *et al.* (LHPC Collaboration), Phys. Rev. Lett. **96**, 052001 (2006).
  - [16] Y. Iwasaki and T. Yoshie, Phys. Lett. B **143**, 449 (1984).
  - [17] C. Allton *et al.* (RBC+UKQCD Collaboration), Phys. Rev. D **76**, 014504 (2007).
  - [18] P. Boyle (RBC+UKQCD Collaboration), Proc. Sci. LATTICE2007 (2007) 005.
  - [19] M. A. Clark and A. D. Kennedy, Phys. Rev. Lett. **98**, 051601 (2007).
  - [20] M. Lin and E. E. Scholz (RBC+UKQCD Collaboration), Proc. Sci. LATTICE2007 (2007) 120.
  - [21] C. Allton *et al.* (RBC+UKQCD Collaboration), arXiv:0804.0473.
  - [22] C. Alexandrou *et al.*, Nucl. Phys. B **414**, 815 (1994).
  - [23] D. Dolgov *et al.* (LHPC and SESAM Collaboration), Phys. Rev. D **66**, 034506 (2002).
  - [24] C. Alexandrou *et al.*, Phys. Rev. D **76**, 094511 (2007).
  - [25] S. Sasaki and T. Yamazaki, arXiv:0709.3150.
  - [26] M. Kim and S. Kim, Phys. Rev. D **58**, 074509 (1998).
  - [27] O. Bar *et al.*, Phys. Rev. D **72**, 054502 (2005).
  - [28] S. Prelovsek, Phys. Rev. D **73**, 014506 (2006).
  - [29] F.-J. Jiang, arXiv:hep-lat/0703012.
  - [30] J.-W. Chen, D. O'Connell, and A. Walker-Loud, arXiv:0706.0035.
  - [31] B. Smigielski and J. Wasem, Phys. Rev. D **76**, 074503 (2007).
  - [32] V. Bernard and U.-G. Meissner, Phys. Lett. B **639**, 278 (2006).